How could 50 °C be reached in Paris: Analyzing the CMIP6 ensemble to design storylines for adaptation

Pascal Yiou, Robert Vautard, Yoann Robin, Nathalie de Noblet-Ducoudré, Fabio D'Andrea, Robin Noyelle

Climate Services 36 (2024) 100518

Contents lists available at ScienceDirect

Climate Services

journal homepage: www.elsevier.com/locate/cliser

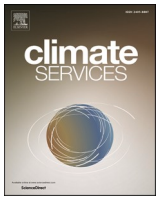

Original research article

How could 50 °C be reached in Paris: Analyzing the CMIP6 ensemble to design storylines for adaptation

Pascal Yiou [a,*], Robert Vautard [a], Yoann Robin [a], Nathalie de Noblet-Ducoudré [a], Fabio D'Andrea [b], Robin Noyelle [a]

[a] Laboratoire des Sciences du Climat et de l'Environnement, UMR8212 CEA-CNRS-UVSQ, IPSL & Université Paris-Saclay, 91191 Gif-sur-Yvette, France
[b] Laboratoire de Météorologie Dynamique, UMR CNRS-X-ENS, IPSL & Université PSL, 75005 Paris, France

ARTICLE INFO

Keywords:
Heatwaves
CMIP6
Model selection
Paris

ABSTRACT

Reaching a surface temperature of 50 °C in a heavily populated region, like Paris, would have devastating effects. Although such a high value seems far from the present-day record of 42.6 °C, its occurrence cannot be dismissed by the end of the 21st century, due to the continuous increase of global mean temperature. In this paper, we address two questions that were asked by the City of Paris to a group of scientists: When does this event start to be likely? What are the prevailing meteorological conditions? We base our study on the CMIP6 simulation ensemble. Many of the CMIP6 yield biases in temperature. Rather than using methods of bias correction, which are not necessarily adapted to high extremes, we propose a pragmatic approach of model selection in order to seek such high temperature events that are deemed realistic. We analyze the meteorological conditions leading to first occurrences of such hot events and their common atmospheric patterns. This paper describes a simple data mining approach (on a large ensemble of climate model simulations) which could be adapted to other regions of the world, in order to help decision makers anticipating and adapting to such devastating meteorological events.

Practical implications

The present study came as a request from the City of Paris, who was interested in the meteorological conditions that would prevail if such high temperatures were reached in Paris. The City of Paris worries, in case of extreme heat in the city, about its capacity to maintain the distribution of water and energy, to carry out emergency procedures such as ambulances, welcome people to the emergency room in hospitals, extinguish starting fires, protect elderly people, and welcome children at school in good conditions. Thus, the City of Paris wanted to set up ad hoc organizational changes prior to reaching such high temperature levels (https://cdn.paris.fr/paris/2023/04/21/paris_a_50_c-le_rapport-Jc4H.pdf). Implementing the work to identify the risks of malfunctioning and to propose adaptation solutions is costly (in time, money and energy). The authors of this paper were solicited to first establish whether such high temperatures could occur in Paris and in which climatic conditions. Once they validated that 50 °C in Paris could occur if the global warming level exceeds 2 °C, stress tests were carried out in some Paris districts in October 2023. Although the City of Paris did not use the exact numbers we produced in this study (e.g., year of occurrence), explaining that such an event could occur during the course of our lifetimes increased the awareness of the public by making it more concrete.

The "real life" stress test findings revealed that to be more resilient, the City of Paris needs to act and invest urgently to lower the temperature impacts of the heat hazard (e.g., with a better water and vegetation management), and the impacts on population (though better monitoring). A resilience plan for Paris is in construction, that gathers all the stakeholders (urban management, water management, health, police). Therefore, the work reported in this paper supports investments to identify the risks of "domino" failures when too many solicitations load the emergency system and to implement a series of adaptation processes to get ready when such an event occurs [https://www.paris.fr/pages/paris-50-c-un-exercice-grandeur-nature-pour-se-preparer-aux-chaleurs-extremes-24322, https://www.lemonde.fr/planete/article/2022/07/16/comment-paris-se-prepare-a-vivre-sous-50-c_6135001_3244.html]. Other French cities like Perpignan (South of France), which are likely to witness such high temperatures before Paris

* Corresponding author.
E-mail address: pascal.yiou@lsce.ipsl.fr (P. Yiou).

https://doi.org/10.1016/j.cliser.2024.100518
Received 28 March 2024; Received in revised form 13 September 2024; Accepted 13 September 2024
Available online 22 September 2024

does, are also interested in such diagnostics [https://madeinperpignan.com/evenement-perpignan-50-degres-climat-eau-biodiversite/].

Even though the computations presented in this paper are conceptually simple, they require extensive computing power and handling complex file formats. If such a study was to be reproduced for other regions or cities, this work could be left to "intermediate entities" (e.g., small and medium enterprises: SMEs) who could use the suite of scripts that we provide on github. Therefore, if data mining for extreme events has an economic value, we present and document tools to achieve it. A French start-up SME is presently working on ways to optimize computations.

Introduction

Heatwaves have huge impacts on society and ecosystems (Bastos et al., 2020; Domeisen et al., 2023; Yin et al., 2023), and frequently generate thousands of extra deaths per summer in Europe. Western European governments took measures to lower vulnerability, after the European heatwaves in 2003. The Pacific North West American heat wave in June 2021 was a shock with temperatures that came close to 50 °C during a couple of days, and were way above previous historical records (Philip et al., 2022). The authorities of a few major cities (in particular in Europe) are in the process of designing adaptation plans to such events, yet unprecedented in Europe, where records since 1950 reach 40–45 °C, except for a few Mediterranean cities (Athens, Syracuse, Cordoba), with record nearing or exceeding 48 °C.

There is no universal definition of a heatwave. In France, Météo France defines a heatwave when day and night temperatures exceed a high threshold (that depends on the region) for more than 3 consecutive days. For safety purposes, *heatwave warnings* can be issued when temperatures can exceed high thresholds, even for short durations. For the Paris area, the threshold values for a "red" warning (leading to conditions similar to those of the summer 2003) are 31 °C during day time (daily maximum temperature: TX) and 21 °C at night (daily minimum temperature: TN). Therefore, there are distinct notions of heat: one is based on the persistence of high temperatures, and the other (which triggers warnings) is based on the intensity only. This paper will focus on the latter.

The city of Paris, with a record (2019) of 42.6 °C, is preparing an adaptation plan to extreme summer temperatures, and a crisis plan for temperatures in the range of 50 °C (Florentin and Lelievre, 2023). Scientific questions that have been asked to the (French) scientific community are:

1. Can temperatures exceed 50 °C in Paris and for how long?
2. What is a likely horizon for the first occurrence of such an event?
3. How are the 50 °C reached?

The record shattering event across Western Canada and the US in 2021 (i.e., at a similar latitude as the Paris area) suggests that one could not dismiss that such a hot event could occur in Europe in years/decades to come. Such temperatures were also observed in southern Europe in 2021 and 2023. Therefore, preparing a crisis exercise and adaptation plans for that level of temperatures is important now, as adaptation actions will take time to be effective.

When daily temperature records are broken, the increments above the previous record are generally a few tenths of degrees. In the Pacific NorthWest American event in summer in 2021, this was called a "record shattering" event because records were broken by several degrees (Fischer et al., 2021). Such record shattering events can be seen as outliers of observed extreme value distributions (Fischer et al., 2023), and hence can be qualified as surprises. Using data from 1950, Philip et al. (2022) estimated a return period for the event of the order of about 1000 year, accounting for the current global warming level. (Bador et al., 2017) have investigated temperature records in regional climate projections. Based on a single climate model, they found the possibility to exceed locally 50 °C in France but not in the Paris region. Here we are interested in hot events that would occur as surprises, similarly to the recent events of 2021 or 2023. Such events are deemed to have a low probability (Philip et al., 2022), which requires large ensemble of data (Bevacqua et al., 2023).

The objective of this article is to present a method that allows analyzing the possibility of temperatures to reach 50 °C in the Paris and provide physically plausible example cases which can serve city managers and planners for adaptation reference using recent climate projections. The recent CMIP6 simulations offer a large multi-model ensemble of data, with several socio-economic scenarios until the end of the 21st century.

This paper also aims at succinctly describing the conditions under which temperatures of 50 °C can be reached in a highly populated European region like Ile-de-France, surrounding Paris (France). We examine the large-scale atmospheric conditions for such an event, and the global warming level above which such conditions are found with significant probabilities in the simulations, accounting for the interannual and interdecadal variability. We mainly describe a data processing chain, and defer a complete physical analysis to another paper.

This description can lead to a *climate service*, to analyze a large ensemble of climate simulations, and provide sensible answers to the challenges outlined in this introduction (Is it possible to reach 50 °C? When? What climatic and meteorological conditions to expect?). The goal is to be able to replicate our analyses easily and change parameters, so that the computations can be transposed to other regions of the planet. Although those data are publicly available, their volume is huge (peta-bytes of data). Treating an ensemble such as CMIP6 requires scientific computer skills and R&D resources, which are rarely available from city practitioners whose main interest is not atmospheric sciences. It is hence deemed useful to propose a simple methodology, easily reproducible by companies providing consulting or climate services, to treat the three challenges outlined above from available data. Hence, this processing chain is intended for entities that are capable of processing climate model data, and communicate results to final stakeholders. To potentially become useful for other cities, such a methodology should be easy to deploy, reproducible and testable on many regions. We however restrict here to the Paris city for the presentation.

Section 2 presents data and models used in this paper. Section 3 describes the first three events that reach 50 °C in the Paris area in three SSP scenarios. This section presents a quick check of the atmospheric conditions that prevail during those events. Section 4 discusses the caveats of the analyses. Section 5 explains practical implications of this paper and how the City of Paris used some of the results. The paper concludes with Section 6.

Data and methods

Data

This analysis uses E-OBS data (Haylock et al., 2008), ERA5 reanalyses (Hersbach et al., 2020) and CMIP6 simulations (Eyring et al., 2016). The CMIP6 simulations include "historical" and four Shared Socioeconomic Pathway (SSP) scenarios (Riahi et al., 2017): 1–2.6, 2–4.5, 3–7.0 and 5–8.5. Historical simulations run from 1860 to 2014, and are constrained by observed forcings (natural and anthropogenic). SSP simulations go from 2015 to 2100 (2300 for some models) and are constrained by economic scenarios of greenhouse gas emissions, pollutants and changes in land use.

Some models provide ensembles of simulations, with slightly perturbed initial conditions. This helps assessing the role of internal climate variability (Deser et al., 2016).

Overall, we considered all simulations that were available to us on August 1st 2023 on the IPSL computing server, which contains a (large) subset of the simulations on the Earth System Grid Federation (ESGF)

that contains all CMIP6 simulations. We used the models for which historical runs and the four SSP scenarios are available. This includes 1288 simulations from 26 climate models. Hence this excludes models with fewer scenario simulations. The ensemble sizes for each model (with historical and four SSP scenario simulations) are indicated in Table 1 below. The ensemble sizes vary from 1 run to more than 50 in SSP simulations, depending on the model. The size of the ensembles also depends on the SSP scenarios.

We considered TX (daily maximum temperature), TG (daily mean temperature) and TN (daily minimum temperature) over France, and SLP (sea-level pressure) over the North Atlantic region, in order to investigate the synoptic conditions during heat events in Paris.

In the selection of models, we removed simulations of the HadGEM3-GC31-HH, HadGEM3-GC31-HM, HadGEM3-GC31-LL, HadGEM3-GC31-LM, HadGEM3-GC31-MH, HadGEM3-GC31-MM, and UKESM1-0-LL models. For those models, the errata documentation for CMIP6 states that: "An issue has been discovered where isolated and irregular events are leading to spikes (a single time step) in the value of surface air temperature lead to the value of daily tasmax[1] datasets in all MOHC simulations that include the atmosphere. Initial investigations on a single simulation suggest that events over 340 K occur once in every 250 days, with events above 350 K occurring once in every 1,200 days. We believe the spikes in tasmax[1] are triggered by the model's surface energy balance, at isolated grid cells, being dominated by sensible heating. For very short periods the accumulated heat appears not to be efficiently mixed away from the surface by the model's sub-grid scale mixing scheme resulting in the spurious values […]". (https://errata.ipsl.fr/static/view.html?uid = 76b3f818-d65f-c76b-bfd8-cae5bc27825c). We checked that the other models we consider do not have such documented issues on temperature.

We extracted TX, TN and TG over the Paris region (Ile de France) outlined in Fig. 1. A bilinear interpolation was performed on the model grid cells over the [1.75–3.25°E; 48.25–49.25°N] region, which includes the administrative area of the City of Paris. This interpolation procedure is necessary because Ile de France can be across several model gridcells, whose size can be much larger (∼2°) than the area of the region itself. When the spatial average across the region is computed, this interpolation allows weighting the model grid cell that cover the Ile de France region. We note that this computation takes ∼ 28 h (for each variable) on the IPSL computing cluster, using 8 parallel CPUs.

We computed the yearly global mean surface temperature (GMST) for each CMIP6 model. The GMST value between 1950 and 2000 is around ∼ 14.1 +/- 0.5 °C (1 sigma) for the CMIP6 historical simulations. The mean GMST in ERA5 for these decades is ∼ 13.5 °C. We determine global warming increase (GWI) as the difference of a 20-year average GMST with the average value at the turn of the 21st century (1950–2000) or at the turn of the 20th century (1850–1900). The latter baseline (from a pre-industrial period) is often used in IPCC reports (IPCC, 2021). In practice, there are three caveats to such a baseline definition: (i) some historical simulations provided on the ESGF servers start in the 20th century, (ii) reanalysis products like ERA5 (Hersbach et al., 2020) or NCEP (Kalnay et al., 1996) start after 1948, which makes data validation difficult, and (iii) a large majority living humans (incl. decision makers) were born after 1950, so that communication from a known baseline is certainly more meaningful. Therefore, we will focus on a definition of "global warming" from a 1950–2000 baseline.

A generic code for extracting time series over a given region from the whole CMIP6 archive is provided on github [https://github.com/pascalyiou/Paris50C.git].

We also used TG from the ERA5 reanalysis (Hersbach et al., 2020) and EOBS (Haylock et al., 2008) data as references to select CMIP6 data (the selection procedure is detailed below). We downloaded the data for the Paris area from the Climate Explorer (https://www.climexp.knmi.

[1] Tasmax is equivalent to TX. The citation is reproduced verbatim.

Table 1
List of CMIP6 models and ensemble sizes for each scenario that are treated in this paper. We only indicate the models for which historical and four SSP scenario runs are available. We excluded the models based on the Met Office Hadley Center (MOHC) model simulations, as they yield documented anomalous behavior for TX. The models in boldface characters are those which pass the Kolmogorov-Smirnov test of a comparison with ERA5 and E-OBS data.

Model	Scenario	Ensemble size	Model	Scenario	Ensemble size
ACCESS-CM2	historical	10	GFDL-ESM4	historical	3
ACCESS-CM2	ssp126	3	GFDL-ESM4	ssp126	1
ACCESS-CM2	ssp245	3	GFDL-ESM4	ssp245	1
ACCESS-CM2	ssp370	3	GFDL-ESM4	ssp370	1
ACCESS-CM2	ssp585	5	GFDL-ESM4	ssp585	1
ACCESS-ESM1-5	historical	40	INM-CM4-8	historical	1
ACCESS-ESM1-5	ssp126	10	INM-CM4-8	ssp126	1
ACCESS-ESM1-5	ssp245	18	INM-CM4-8	ssp245	1
ACCESS-ESM1-5	ssp370	10	INM-CM4-8	ssp370	1
ACCESS-ESM1-5	ssp585	40	INM-CM4-8	ssp585	1
AWI-CM-1–1-MR	historical	5	INM-CM5-0	historical	10
AWI-CM-1–1-MR	ssp126	1	INM-CM5-0	ssp126	1
AWI-CM-1–1-MR	ssp245	1	INM-CM5-0	ssp245	1
AWI-CM-1–1-MR	ssp370	5	INM-CM5-0	ssp370	5
AWI-CM-1–1-MR	ssp585	1	INM-CM5-0	ssp585	1
BCC-CSM2-MR	historical	3	**IPSL-CM6A-LR**	historical	33
BCC-CSM2-MR	ssp126	1	**IPSL-CM6A-LR**	ssp126	6
BCC-CSM2-MR	ssp245	1	**IPSL-CM6A-LR**	ssp245	11
BCC-CSM2-MR	ssp370	1	**IPSL-CM6A-LR**	ssp370	11
BCC-CSM2-MR	ssp585	1	**IPSL-CM6A-LR**	ssp585	7
CAMS-CSM1-0	historical	1	KACE-1–0-G	historical	3
CAMS-CSM1-0	ssp126	1	KACE-1–0-G	ssp126	3
CAMS-CSM1-0	ssp245	1	KACE-1–0-G	ssp245	3
CAMS-CSM1-0	ssp370	1	KACE-1–0-G	ssp370	3
CAMS-CSM1-0	ssp585	1	KACE-1–0-G	ssp585	3
CanESM5	historical	50	**MIROC-ES2L**	historical	31
CanESM5	ssp126	50	**MIROC-ES2L**	ssp126	3
CanESM5	ssp245	50	**MIROC-ES2L**	ssp245	30
CanESM5	ssp370	50	**MIROC-ES2L**	ssp370	1
CanESM5	ssp585	50	**MIROC-ES2L**	ssp585	2
CMCC-ESM2	historical	1	MIROC6	historical	50
CMCC-ESM2	ssp126	1	MIROC6	ssp126	50
CMCC-ESM2	ssp245	1	MIROC6	ssp245	50
CMCC-ESM2	ssp370	1	MIROC6	ssp370	3

(*continued on next page*)

Table 1 (*continued*)

Model	Scenario	Ensemble size	Model	Scenario	Ensemble size
CMCC-ESM2	ssp585	1	MIROC6	ssp585	50
CNRM-CM6-1	historical	30	**MPI-ESM1-2-HR**	historical	10
CNRM-CM6-1	ssp126	1	**MPI-ESM1-2-HR**	ssp126	2
CNRM-CM6-1	ssp245	1	**MPI-ESM1-2-HR**	ssp245	2
CNRM-CM6-1	ssp370	3	**MPI-ESM1-2-HR**	ssp370	10
CNRM-CM6-1	ssp585	1	**MPI-ESM1-2-HR**	ssp585	2
CNRM-ESM2-1	historical	10	MPI-ESM1-2-LR	historical	31
CNRM-ESM2-1	ssp126	1	MPI-ESM1-2-LR	ssp126	10
CNRM-ESM2-1	ssp245	1	MPI-ESM1-2-LR	ssp245	10
CNRM-ESM2-1	ssp370	3	MPI-ESM1-2-LR	ssp370	10
CNRM-ESM2-1	ssp585	1	MPI-ESM1-2-LR	ssp585	30
EC-Earth3	historical	73	**MRI-ESM2-0**	historical	12
EC-Earth3	ssp126	2	**MRI-ESM2-0**	ssp126	1
EC-Earth3	ssp245	30	**MRI-ESM2-0**	ssp245	9
EC-Earth3	ssp370	52	**MRI-ESM2-0**	ssp370	5
EC-Earth3	ssp585	58	**MRI-ESM2-0**	ssp585	5
EC-Earth3-Veg	historical	9	NorESM2-LM	historical	3
EC-Earth3-Veg	ssp126	5	NorESM2-LM	ssp126	1
EC-Earth3-Veg	ssp245	6	NorESM2-LM	ssp245	3
EC-Earth3-Veg	ssp370	4	NorESM2-LM	ssp370	3
EC-Earth3-Veg	ssp585	8	NorESM2-LM	ssp585	1
EC-Earth3-Veg-LR	historical	3	**NorESM2-MM**	historical	3
EC-Earth3-Veg-LR	ssp126	3	**NorESM2-MM**	ssp126	1
EC-Earth3-Veg-LR	ssp245	3	**NorESM2-MM**	ssp245	2
EC-Earth3-Veg-LR	ssp370	3	**NorESM2-MM**	ssp370	1
EC-Earth3-Veg-LR	ssp585	3	**NorESM2-MM**	ssp585	1
FGOALS-g3	historical	5	TaiESM1	historical	1
FGOALS-g3	ssp126	4	TaiESM1	ssp126	1
FGOALS-g3	ssp245	4	TaiESM1	ssp245	1
FGOALS-g3	ssp370	5	TaiESM1	ssp370	1
FGOALS-g3	ssp585	4	TaiESM1	ssp585	1

nl).

In order to assess the potential role of large-scale climate variability we computed from the CMIP6 archive:

- an El Niño 3.4 index (Trenberth, 1997) based on sea-surface temperature (SST) in the Central Equatorial Pacific (5 N-5S, 170 W-120 W). This index was computed from monthly anomalies of spatial averages of SST. Positive values of the Niño3.4 index correspond to El Niño episodes.
- An Atlantic Multi-decadal Oscillation (AMO) index (Kerr, 2005) based on SST in the North Atlantic region. This index was computed as a spatial average (80 W-0E; 0–60 N) of monthly SST. The global SST mean value was subtracted in order to remove long term trends.

These two indices account for most of the interannual large scale variability of climate.

Pre-processing

All CMIP6 models are prone to biases, in particular due to their horizontal resolution (Carvalho et al., 2021), which leads to a misrepresentation of several processes which are relevant to reproduce the energy balance near the surface (Domeisen et al., 2023). One way to solve this issue is to use bias correction methods (Maraun and Widmann, 2018). Such an approach requires a "sound" reference, like a very high-resolution reanalysis (e.g., SAFRAN (Quintana-Segui et al., 2008)), which is not necessarily available everywhere in the world. In addition, such bias correction methods are rather computer costly, and have only been performed on a small subset of CMIP6 (e.g., only one member per model/group, for arbitrarily selected models). Finally, the bias correction of each individual simulation crunches model statistics towards the statistics of one realization of the true climate variability over a limited time period (the correction training period), the observed one, and may thus artificially reduce the simulated natural variability. This effect can be particularly exacerbated for extremes, because the interdecadal variability at regional scale can be large.

We chose here an alternative approach consisting of selecting models yielding the smallest biases over Ile de France of the "historical" simulation for TG, taking advantage of the large number of simulations available in CMIP6. We made a comparison of TG in historical CMIP6 model simulations with ERA5 and EOBS between 1995 and 2014. We performed a Kolmogorov-Smirnov (k-s) test (von Storch and Zwiers, 2001) between each historical simulation, and ERA5 (and EOBS), to compare the probability distributions of daily summer TG in CMIP6 models and reanalyses or EOBS. The threshold we consider for the k-s test value is 0.1. We opted for an "inclusive" approach for model selection: the whole ensemble of one model is kept when at least one member yields a TG probability distribution between 1995 and 2014 that is similar to ERA5 *or* EOBS.

There are two reasons for this strategy:

1. As stated earlier, there is a small offset between TG in ERA5 and EOBS for the Paris area, which means that ERA5 would not pass the Kolmogorov-Smirnov test if EOBS was chosen as a reference (and vice versa). There is no reason to favor EOBS over ERA5, which does not include information in Paris *intra muros* (e.g., the Paris Montsouris station), and it is reasonable to compare CMIP6 with a climate model simulation that best resembles observations, such as a reanalysis product.
2. If a CMIP6 model yields an ensemble to sample internal variability, some of its members could be different from an observation reference during a 20-year period, because model years are not "real world" years. But we do not want to reject them, because if one member is satisfactory, it suggests that the model is able to reproduce observations over a 20-year period of time, so that scenario simulations could bring relevant information. Some models come with only one run, so that this test might exclude them if this only run does not pass a statistical test with observations. This encourages large ensemble approaches, as discussed by Bevacqua et al. (2023).

This selection procedure obviously contains arbitrary elements (k-s test threshold, length of time series for comparisons, period of comparison, reference data, choice of variable for comparison). In a preliminary study (in French: https://grec-idf.eu/simulations-paris-50c/), we used a different selection procedure (which was based on tests on TX rather than TG, and removed simulations that did not pass the test). This led to a somewhat different (smaller) ensemble of models, but the overall results in terms of first occurrence and global warming were similar. This suggests a robust behavior of this pre-processing step.

As it is, this procedure selects 819 of the available 1288 simulations

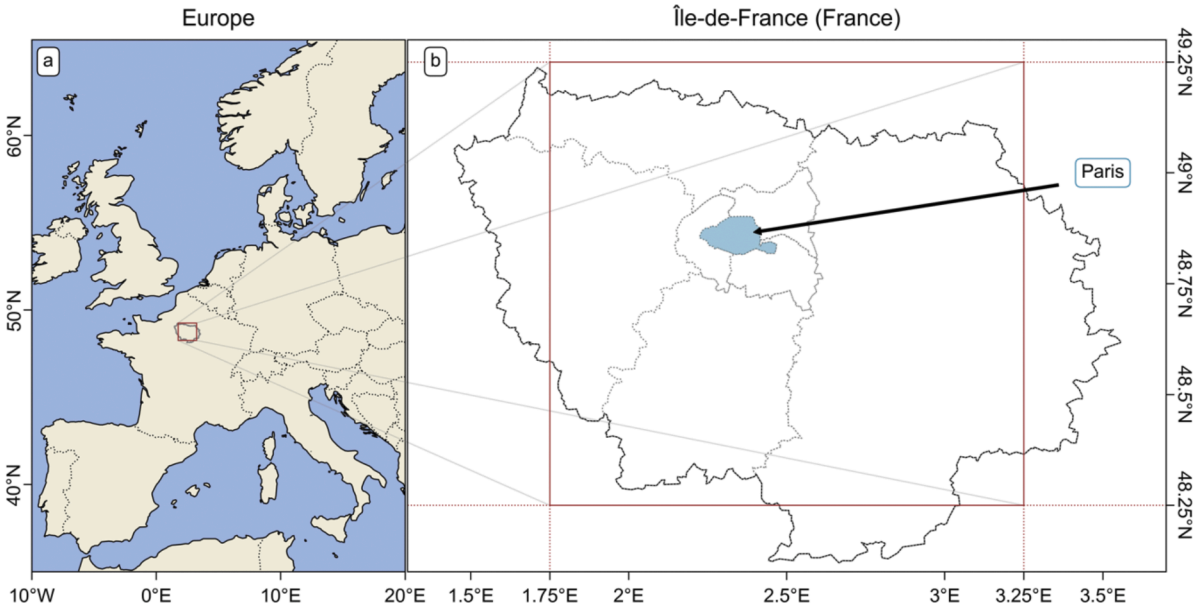

Fig. 1. Ile de France Area in Western Europe (panel a). The red rectangle in panel b refers to the region that is considered in the model and reanalysis data. Paris "intra-muros" is indicated in blue.

(with 585 SSP simulations), and 12 of the 26 CMIP6 models (outlined in boldface in Table 1).

Selection of events

An event exceeding 50 °C is potentially very local and short lived, with an amplification by urbanization and surface water availability. We consider a small region that averages urban areas (Paris *intra-muros*) and suburban areas with forests. Due to the urban heat island effect, we estimate that 50 °C can be exceeded within Paris, when TX exceeds 48 °C over the Ile-de-France area. This assumption is justified by computing the differences of TX between observation at Paris-Montsouris station, and the average over the Ile de France region (Fig. 2). There is a systematic offset between TX in Paris-Montsouris and the average over the Paris area when TX exceeds 35 °C. Therefore, we consider that TX exceeds 50 °C in Paris when TX exceeds 48 °C over Ile de France. This empirical threshold could be modified. We also verified that for extreme heat days, this temperature variation is typical of intra-region variations, over the last 10 years for which we could have access to more stations (from https://www.infoclimat.fr).

From a list of 12 models and 585 simulations, we identified the years with at least one exceedance of 48 °C before 2100. The results are

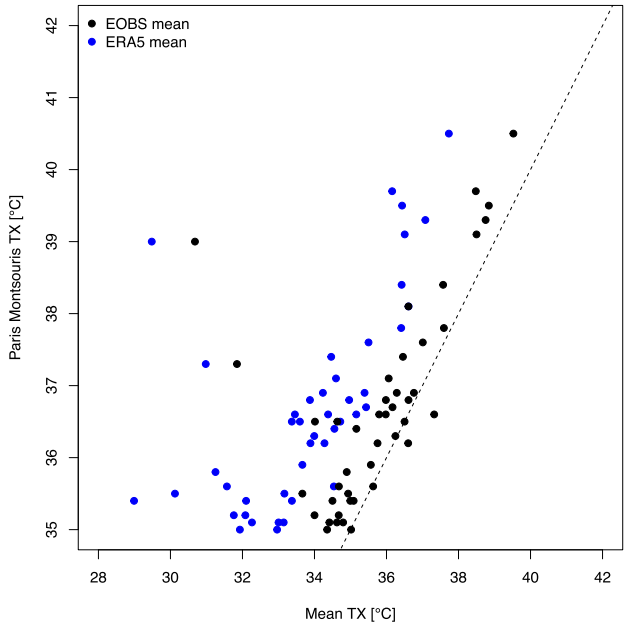

Fig. 2. Scatter plot of TX in Paris Montsouris versus the average of TX over the region outlined in Fig. 1, when TX exceeds 35 °C in Paris Montsouris. The averages are computed from the EOBS (black circles) data and the ERA5 reanalysis (blue circles) data. The dashed line is the diagonal line.

Table 2
List of models with at least one simulation that exceeds 48 °C in Paris at least for one day. We indicate the year of the first occurrence of TX>48 °C among all members of the same scenario. The fifth column indicates the global surface temperature (GMST in °C) when the event occurs. The sixth column indicates the GMST difference (GWI, in °C) with a 1950–2000 baseline. The three simulations that are discussed in the results section are outlined in boldface.

Model name	Scenario	#members with TX>48 °C/ #Available members	First year with TX>48 °C	GMST (°C)	GWI (°C)
CanESM5	ssp370	12/50	2079	18.6	3.5
CanESM5	ssp585	23/50	2071	19.2	3.9
CMCC-ESM2	**ssp245**	**1/1**	**2077**	**17.3**	**2.8**
CMCC-ESM2	ssp370	1/1	2071	17.3	2.8
CMCC-ESM2	**ssp585**	**1/1**	**2049**	**16.7**	**2.1**
ACCESS-CM2	ssp370	1/3	2099	18.8	4.1
EC-Earth3-AerChem	ssp370	1/1	2098	19.1	5.1
EC-Earth3-CC	ssp585	1/1	2093	19.6	4.9
EC-Earth3	ssp370	4/52	2094	18.6	3.4
EC-Earth3	ssp585	29/58	2080	18.5	3.5
EC-Earth3-Veg-LR	**ssp370**	**1/3**	**2058**	**16.3**	**2.7**
EC-Earth3-Veg-LR	ssp585	1/3	2094	19	5.4
EC-Earth3-Veg	ssp585	1/8	2091	18.9	4.6

summarized in Table 2 (not all model simulations in Table 1 reach 48 °C before 2100).

Results

Event occurrence in CMIP6

We find that 8 models, among those selected to be realistic, exceed, at least once, 48 °C between 2020 and 2100. Fig. 3 and Table 2 report models for which at least one member in one scenario yields a TX>48 °C event. Those 8 models produced 232 simulations. Among this ensemble, 81 simulations yield at least one TX>48 °C event (third column in Table 2).

We first consider the four SSP separately. For illustration purposes, we select the model simulations with the earlier dates that reach 48 °C in the Paris area. We find that TX never exceeds 48 °C in the SSP1-2.6 scenario. Therefore, we focus on SSP2-4.5, SSP3-7.0 and SSP5-8.5 (Fig. 3). Only CMCC-ESM2 reaches the threshold with SSP2-4.5 (Fig. 3a). This model was run with only one member.

We computed the GMST increase (GWI) of the decades around each event since a 1950–2000 baselines. From Fig. 4, it appears that TX>48 °C events in CMIP6 simulations occur when the GWI exceeds 2 °C.

Most of the selected CMIP6 simulations (with 2 exceptions) do not reach this threshold as long as the GMST does not exceed 16 °C (Fig. 3), which correspond to a GWI of about 2.5 °C since 1950–2000 (Fig. 4). As reaching this temperature is physically possible (Noyelle et al., 2023b; Zhang and Boos, 2023), those simulations will be discussed in this paper.

There is a shift of CMIP6 model behavior with SSP3-7.0, where 6 models reach the 48 °C threshold between 2079 and 2100 (i.e., within the expected lifetime of the junior authors of this paper). The GWI for those models is larger than 2.7 °C (with respect to a 1950–2000 baseline: Fig. 4).

With SSP5-8.5, eight models reach the 48 °C threshold between 2049 and 2100, with GWI warming larger than 2.1 °C (with respect to a 1950–2000 baseline). Two models (CMCC-ESM5 and EC-Earth-Veg-LR) reach this threshold before 2055 (i.e., within the expected lifetime of the senior authors of this paper).

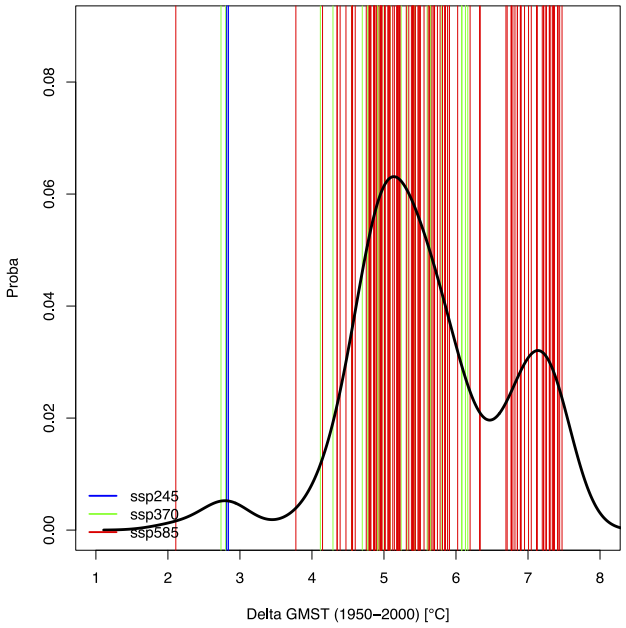

Fig. 4. Distributions of GMST increase (GWI) values when TX>48 °C in Paris, from reference baselines of GMST in 1950–2000. The vertical bars indicate all occurrences of TX>48 °C. The colors indicate the SSP scenario of the TX>48 °C event occurrences. The black line is an empirical probability density function of the year of occurrence of TX>48 °C.

We pooled all 81 simulations for which TX exceeds 48 °C and estimated an empirical probability function for GWI values from a 1950–2000 baseline. The empirical probability was weighted by the total number of considered simulations (232). This gives a crude idea of the probability to exceed the 48 °C threshold for GWI levels of warming. There are more sophisticated ways of obtaining such probabilities, in particular using Extreme Value Theory (Coles, 2001; Robin and Ribes, 2020). We defer such analyses to a future paper.

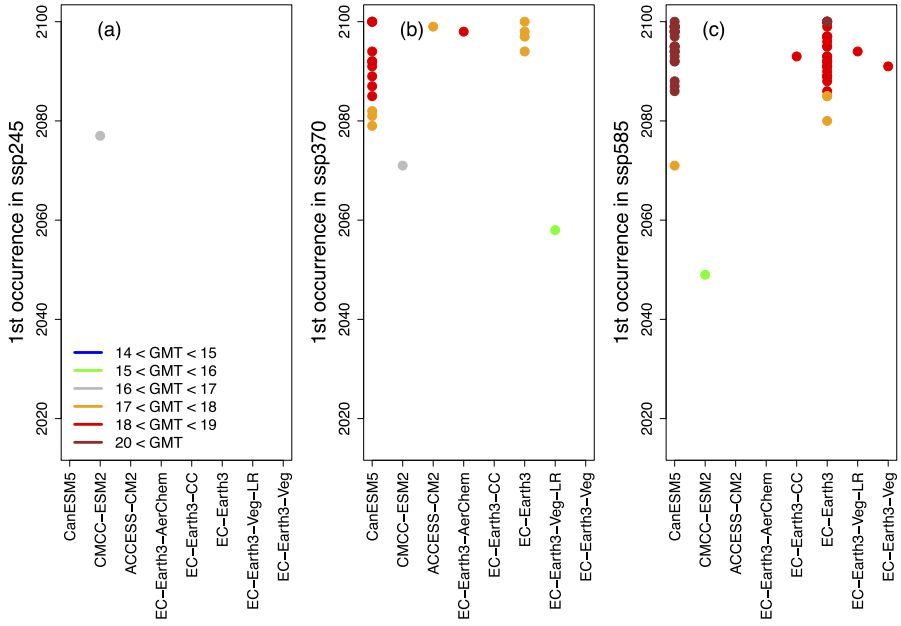

Fig. 3. Time of first exceedance of 48 °C in CMIP6 models for three SSP scenarios. The vertical axis indicates the year of first occurrence of TX>48 °C in the Ile-de-France region, including Paris in model simulations. TX can exceed 48 °C at later years, but this is not reported in the figure. The colors indicate the GMST for the 20 years around the year of TX>48 °C (panel (a) for legend).

We notice in Fig. 4 (black line) that a peak probability is obtained when GWI (from 1950 to 2000) is around 5 °C (around 6 % chance). If GWI is lower than 2 °C, this probability is negligible. It becomes measurable (1 % chance) when GWI reaches ∼ 2.7 °C. The reasoning behind this statement is that one needs more than 10^4 years of data in order to sample events of probability $\approx 10^{-2}$. With our selection procedure, we have an ensemble of ≈ 49000 years of simulations. Due to the nonstationarity of the simulations, we estimate that probabilities higher than $\approx 10^{-2}$ can be detected.

Large-scale variability

The rationale for using ensembles from a multi-model suite of climate models was to sample large-scale climate variability. El Niño and Atlantic multi-decadal variability are major modes that are likely to affect long term variability. Niño3.4 and AMO indices were computed for the simulations of the 8 models for which TX>48 °C occurs before 2100, for all scenarios.

Fig. 5 shows the June-July-August (JJA) averages of the two indices in all simulations (historical and scenarios). Note that the AMO index values are positive in the summer (and negative in the winter) and are not centered around 0 values.

We find that the TX>48 °C events that are outlined in Fig. 3 generally occur when the two large-scale indices are above average, i.e., during El Niño patterns and high AMO. This is consistent across the detected events, among the 8 considered climate models. North Atlantic warm temperatures indeed tend to favor a warm summer background.

Daily summer variations for heat events

We select the first occurrence of TX>48 °C for each SSP scenario. We hence retain CMCC-ESM2 for SSP2-4.5, EC-Earth3-Veg-LR for SSP3-7.0 and CMCC-ESM2 for SSP5-8.5 (Table 2). This choice is obviously arbitrary from the physical point of view. For illustration purposes, we will focus on the earliest occurrences, i.e., the events that the authors of this paper are likely to witness.

The summer time series of daily TX and TM (from June 1st to August 31st) are shown in Fig. 6 for the three selected model, along with the already experienced extremes of 2003 and 2022. Apart from the TX>48 °C peaks, the distributions of temperatures are within the variations observed during the hot summers of 2003 and 2022, which shows that the whole summers are already warm. As stated in the Introduction, Météo-France defines a heatwave ("canicule") in Paris when TX exceeds 31 °C and TN exceeds 21 °C [https://meteofrance.com/actualites-et-dossiers/comprendre-la-meteo/canicule-vague-ou-pic-de-chaleur]. Such a definition depends on the region, with higher thresholds in the Southern part of France. Due to the urban effects that were identified before, we can lower such a threshold to 29 °C for TX, as rough estimates over the Paris region. We retain a 20 °C threshold for TN, as it defines tropical nights.

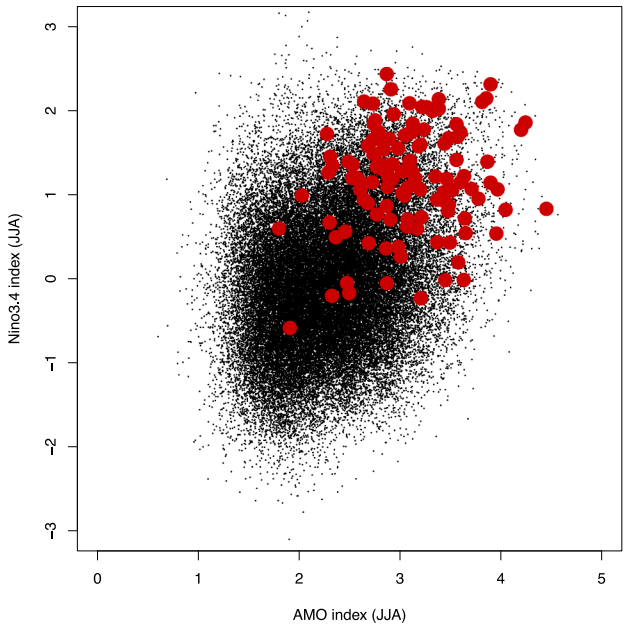

Fig. 5. Scatter plot of Niño3.4 and AMO indices for the model simulations in Table 2, for June-July-August. The red circles indicate the values when a TW>48 °C event occurs.

We find that reaching a 48 °C peak is obtained during warm summers (according to present-day standards: Fig. 6), with a large number of days above the mean seasonal cycle. During those summers the values of TX exceed 29 °C and TN exceed 20 °C on several occasions, which means that several heatwaves (similar to those of 2003 and 2022) also occur during the course of those summers. The peaks of TX>48 °C correspond to TX anomalies of more than 20 °C above the present-day seasonal cycle and last for one day.

The selected simulations show periods of tropical nights (i.e., when the minimal daily temperature TN exceeds 20 °C). We note that the warmest tropical nights do not necessarily occur on the same day as the warmest TX, although tropical nights do occur when TX is high.

TX and SLP patterns

This section serves as a quick check that the climate simulation data are "fit for purpose" and do not yield obvious errors. Systematic process studies are deferred to other papers (D'Andrea et al., 2024; Noyelle et al., 2023b, a).

The temperature patterns over France and the atmospheric circulation (SLP) patterns over the Eastern North Atlantic during the three events are shown in Fig. 7 to Fig. 9. SLP anomalies are computed with respect to the summer (June-July-August) average for each SSP scenario.

For SSP2-4.5, we selected the CMCC-ESM5 model. The TX>48 °C event occurs in July 2077, with a GWI of ∼ 2.3 °C. The maximum TX pattern is near the Paris region and TX exceeds 40 °C over most of France (Fig. 7a). Therefore, the heat event over Paris is also obtained for many gridcells of the model around the Paris region. The atmospheric circulation pattern shows an anticyclone over Scandinavia, and lows over France and west of France (Fig. 7b). This atmospheric pattern also corresponds to observed heatwaves of 2003 (Yiou et al., 2021) and 2022 in France (Herrera-Lormendez et al., 2023; Ibebuchi and Abu, 2023). The peaks of temperature were reached in August 2003 and July 2022, after persisting anticyclonic (blocking) atmospheric pattern above Scandinavia (more than 2 weeks), and drought conditions. Such atmospheric patterns correspond to the most intense heatwaves that could occur in the Paris area (Noyelle et al., 2023a).

For SSP3-7.0, we selected the EC-Earth3-Veg-LR model. TX exceeds 48 °C on the 16th of August 2077 in the r3i1p1f1 member, i.e. after the apex of the seasonal cycle. The GWI from 1950 to 2000 is ∼ 2.7 °C. The center of the extreme TX pattern is located in North East France (Fig. 8a). The hot pattern covers most of France, with TX values above 40 °C over most of the country. The atmospheric circulation shows an anticyclonic pattern between Iceland and Scandinavia and in Central Europe. The circulation yields a strong cyclonic pattern west of Ireland (Fig. 8b). Such a pattern is likely to convey warm air from North Africa into France.

For SSP5.8–5, the early TX>48 °C event occurs in July 2049 in CMCC-ESM2 with a GWI of ∼ 2.1 °C (since 1950–2000). The center of the event occurs in the South West of France, with temperatures exceeding 50 °C (Fig. 9a). Most of the country yield TX over 42 °C. Northern Spain is also affected by high temperatures. The heat does not extend to the east of France. The atmospheric circulation pattern yields

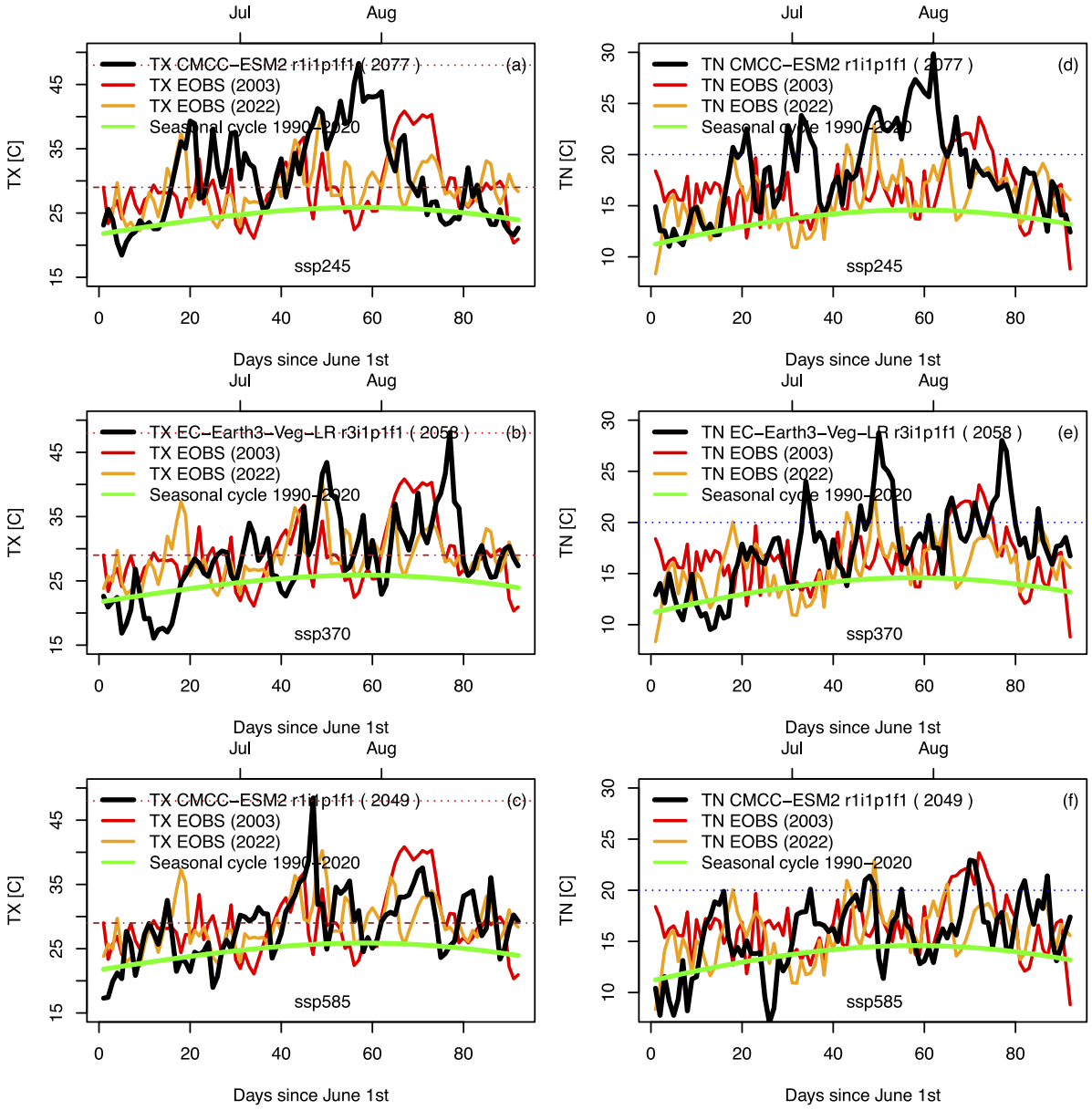

Fig. 6. Time series of daily maximum (TX: left column) and minimum (TN: right column) temperatures in the Paris area for three scenarios. Black lines indicate TX and TN in models. Red and orange lines indicate TX and TN in EOBS for the summers of 2003 and 2022 (respectively). The horizontal red dotted line indicates the 48 °C threshold for TX. The horizontal dashed brown lines indicate the 29 °C TX threshold for heatwaves. The horizontal blue dotted line indicates 20 °C (TN threshold for tropical nights). The green lines indicate the seasonal cycle for TX and TN, computed from the EOBS data (1990–2020).

an anticyclonic feature east of France (centered over the Balkans), and a depression between Iceland and Brittany (Fig. 9b). In both cases, the presence of a depression on the west side of the heatwave likely increases temperature over France via southerly advection or diabatic heating in the frontal area (Domeisen et al., 2023).

Out of those three events (from three SSP scenarios, and three different climate models), three events occur with a GWI between 2.1 °C and 2.8 °C. Those three events yield atmospheric patterns that are reminiscent of already observed heatwaves in Paris, albeit with exacerbated TX values.

Discussion

This paper presents a simple approach to outline extreme temperature events in a large urban and sub-urban region surrounding (and including) Paris. The methodology is based on data inspection and does not contain any sophisticated statistical (Parey, 2008; Yiou and Jézéquel, 2020) or physical (Gessner et al., 2021; Ragone et al., 2018) modelling approaches. Those results serve as a first step for further in-depth studies of extreme heatwaves.

Many choices have been subjective (or based on previous experience): threshold of temperature daily increments, global covariate, and general frequency of extremes. The results were obtained on the IPSL computing facility, for which a (large) subset of the simulations of CMIP6 are available. The same computations are possible with access to Earth System Grid Federation (ESGF) servers throughout the world, although they would require downloading a large amount of data.

We have identified events corresponding to moderate GMST increase (between 2.1 and 2.8 °C). Those events come with spates of tropical nights (minimum temperatures over 20 °C), which would exacerbate the impacts on health of exceeding 50 °C during the day. Some of the Paris events correspond to larger scale events, where temperature exceeds

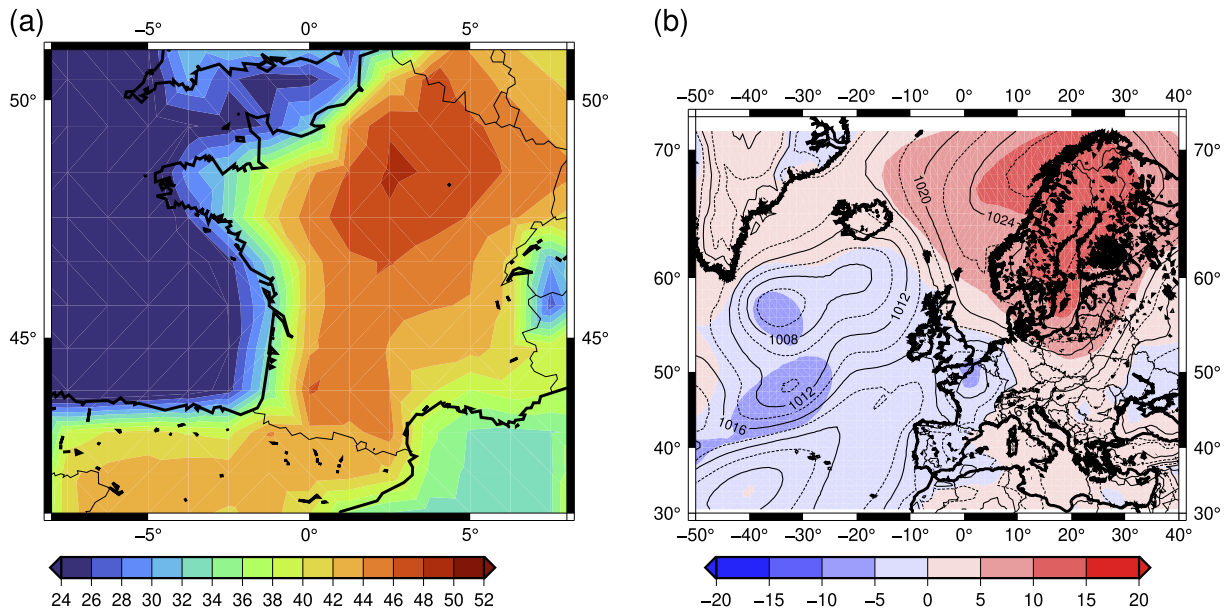

Fig. 7. TX over France (panel a) and SLP over the North Atlantic (panel b) on 27 July 2077, for CMCC-ESM2, in SSP2-4.5 (r1i1p1f1). TX (panel a) is expressed in °C. SLP is expressed in hPa (isolines in panel b). Colors in panel (b) correspond to anomalies of SLP (in hPa) with respect to the summer average.

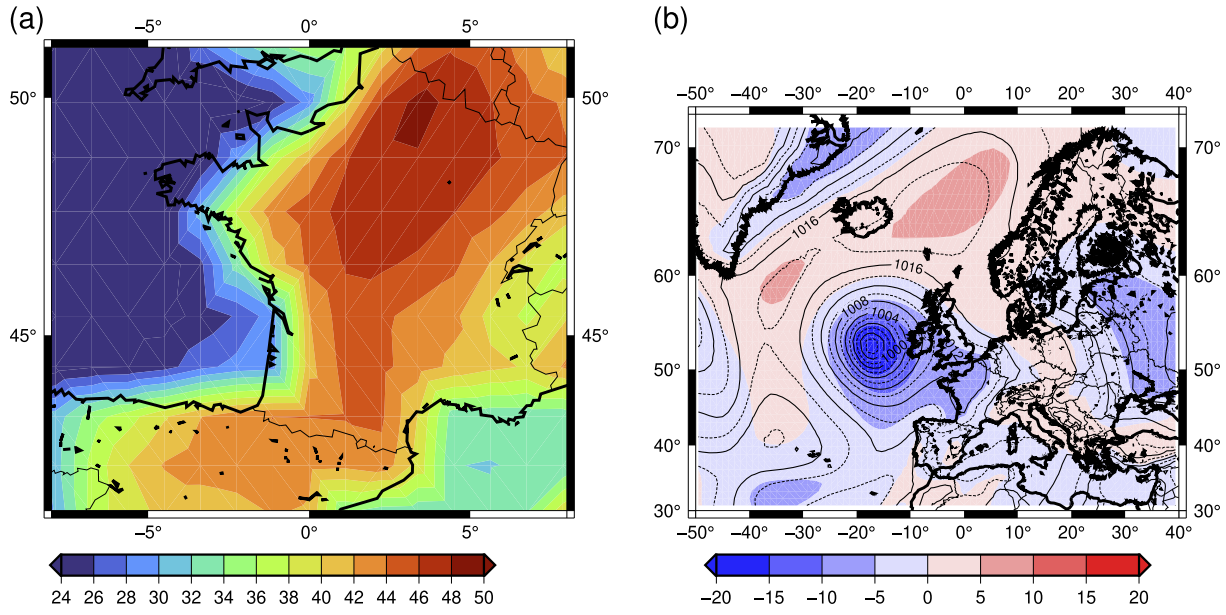

Fig. 8. TX over France (panel a) and SLP over the North Atlantic (panel b) on 16 August 2058, for EC-Earth3-Veg-LR, in SSP3-7.0 (r3i1p1f1). TX (panel a) is expressed in °C. SLP is expressed in hPa (isolines in panel b). Colors in panel (b) correspond to anomalies of SLP (in hPa) with respect to the summer average.

50 °C (e.g., in the south west of France) and large parts of the country have TX above 40 °C. Therefore, a crisis in Paris would also be reflected in other regions of France, where temperatures could even be higher, especially in urban areas (in Amiens: Fig. 8a; or in Bordeaux: Fig. 9a). We have not quantified the probability of exceeding this high threshold, because it is rarely observed more than once in each simulation. This probability is deemed to be negligible for a global surface temperature increase lower than 2 °C within the next two decades. It increases to ∼ 1 % chance if the global surface temperature increases by 2.7 °C. Yet, it cannot be excluded, because Western Europe warms faster than the rest of the world (Rousi et al., 2022; Vautard et al., 2023), and temperature has already reached 48.8 °C in Sicily (Southern Italy) in August 2023. If global surface temperature (GMST) increases by more than 4 °C since 1950–2000, the probability of such hot events increases dramatically in the CMIP6 database.

We have not discussed in detail the mechanisms leading to hot extremes in Paris, which is left for further studies. We have shown that the prevailing large-scale conditions during those hot events correspond to El Niño states and intense AMO. Such large-scale features tend to increase surface temperature over the northern midlatitudes (Kerr, 2005; Trenberth, 1997). This result is not surprising as it explains the "background" warm summer temperatures outlined in Fig. 6.

Several studies have shown that the mechanisms leading to hot summer temperatures in the midlatitudes are connected to (i) adiabatic warming due to atmospheric subsistence, (ii) diabatic warming due to shortwave radiation, sensible and latent heat fluxes, and (iii) Advection of warm air from neighboring regions (Domeisen et al., 2023; Röthlisberger and Papritz, 2023). The first mechanism is linked to an

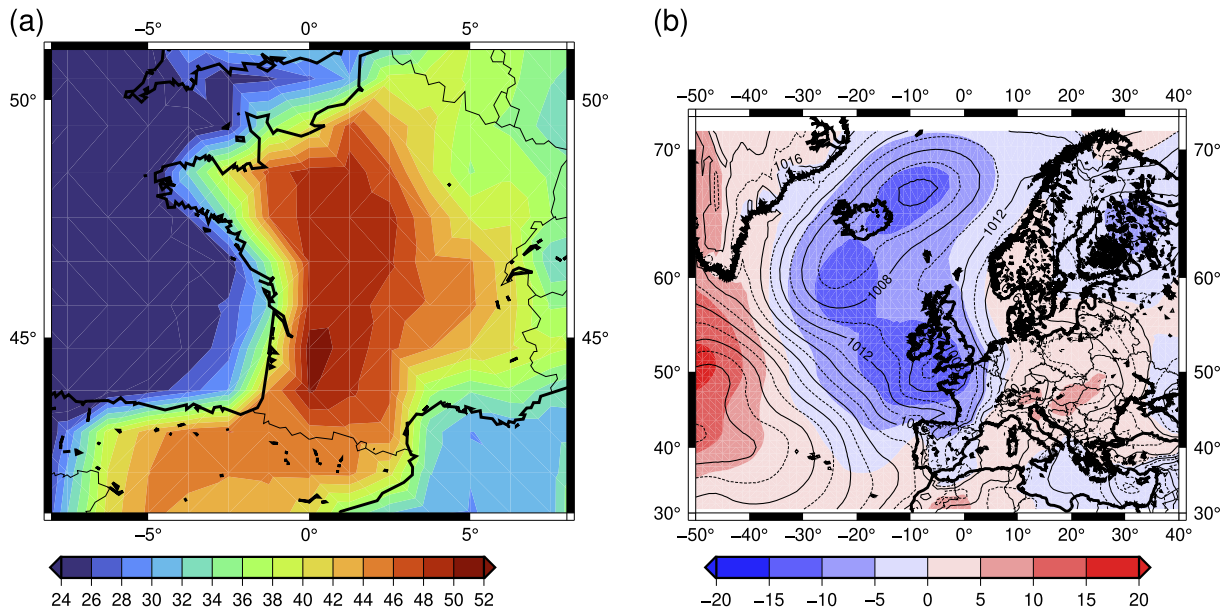

Fig. 9. TX over France (panel a) and SLP over the North Atlantic (panel b) on 17 July 2049, for CMCC-ESM2, in SSP5-8.5 (r1i1p1f1). TX (panel a) is expressed in °C. SLP is expressed in hPa (isolines in panel b). Colors in panel (b) correspond to anomalies of SLP (in hPa) with respect to the summer average.

anticyclonic system and explains half of the high temperature anomalies in present-day climate (Röthlisberger and Papritz, 2023). Hence, the high temperature found with the CMCC-ESM2 simulation in SSP2-4.5 is coherent with this scenario. The high temperature in the two other examples (EC-Earth3-Veg-LR, SSP3-7.0 (r3i1p1f1); CMCC-ESM2, in SSP5-8.5 (r1i1p1f1)) correspond to a mechanism of warm air advection, due to the strong cyclonic circulation west of France. The rather short duration of the T>48 °C events in the three cases (only one day), which are followed by a strong temperature drop (albeit to still hot values) correspond to a limiting mechanisms of convection developed by (Noyelle et al., 2023b; Zhang and Boos, 2023). The verification of such mechanisms requires atmospheric data on several geopotential heights, which are not available in all CMIP6 simulations. Surface precipitation alone does not provide enough information. Hence, a systematic investigation of the physical mechanisms leading to such high temperatures, and how those mechanisms are affected by climate change, requires many "manual" verifications on the available data files, which are beyond the scope of this paper.

Conclusion

This paper aims at exploring how a temperature of 50 °C could be reached in the Paris area, by examining the CMIP6 database. The general questions that were asked by the City of Paris where: when? what level of global warming? What type of meteorology? Exploring the CMIP6 database poses a few statistical, physical and computing challenges that are tackled in the paper.

This paper is meant to provide an automated data-processing chain for the analysis of extremes in this simulation ensemble, with an illustration for the Paris area. This serves as a demonstrator for a climate service for policymakers, which can be transposed to other regions in the world. The important points of this data mining demonstrator are:

1. the reproducibility of the diagnostics, so that the analyses could be replicated on climate projection updates for the upcoming IPCC report,
2. the facilitated transposition to other places in the world (e.g., the City of Perpignan, France: https://madeinperpignan.com/evenement-perpignan-50-degres-climat-eau-biodiversite/).

One of the salient points for decision makers of our analysis is the estimate of the probability of exceeding high temperature thresholds as a function of the global mean temperature increase. If the detection threshold is lowered to 46 °C (which is not far from the present record in Paris: 42.6 °C at Paris-Montsouris in 2019), more models are selected (11 vs. 8 for 48 °C), and the probability of exceeding this threshold for a GMST increase of 2–4 °C since 1950–2000 is multiplied by a factor of 2 (not shown).

A major caveat of this automated data mining analysis is that it is necessary to check manually that the climate model simulations do not contain hard-to-detect mistakes or biases, such as the numerical instabilities of the UKESM model (but not limited to this model), which are documented in https://errata.ipsl.fr/static/index.html (among other official sites).

We do not propose a complete climate analysis of the events (which would be an entire paper by itself) and focus on extremely simple diagnostics. Hence this data-processing chain can serve as a preliminary step to identify relevant (in the sense that was defined in the methods section) simulations, and avoid sophisticated (and computer costly) steps of bias correction.

CRediT authorship contribution statement

Pascal Yiou: Writing – review & editing, Writing – original draft, Software, Methodology, Investigation, Formal analysis. **Robert Vautard:** Writing – review & editing, Writing – original draft, Methodology, Investigation, Funding acquisition, Conceptualization. **Yoann Robin:** Writing – review & editing, Visualization, Data curation. **Nathalie de Noblet-Ducoudré:** Writing – review & editing, Funding acquisition, Conceptualization. **Fabio D'Andrea:** Writing – review & editing, Conceptualization. **Robin Noyelle:** Writing – review & editing, Investigation.

Declaration of competing interest

The authors declare that they have no known competing financial interests or personal relationships that could have appeared to influence the work reported in this paper.

Data availability

Public links to the data are provided in the manuscript

The codes (in R, cdo and shell scripts) to perform all data processing computations is available from https://github.com/pascalyiou/Paris50C.git.

The CMIP6 data files are available from the IPSL ESGF node: https://esgf-node.ipsl.upmc.fr/projects/esgf-ipsl/

ERA5 reanalysis and E-OBS data sets were retrieved from the Climate Explorer: https://climexp.knmi.nl/ . We extracted tasmax and tasmin over the region outlined in Fig. 1, directly from the Climate Explorer.

Acknowledgements

This paper was motivated by the Groupe régional d'expertise sur le changement climatique et la transition écologique (GREC) in Île-de-France. We thank the ESPRI computing mesocenter at IPSL for making the CMIP6 data available. We thank Olivier Boucher (LMD) for discussions on the choices of parameter of the computer scripts, and checking the reproducibility of the results.

Funding sources

This paper received the support of the grant ANR-20-CE01-0008-01 (SAMPRACE) and from Agence Nationale de la Recherche - France 2030, as part of the PEPR TRACCS programme under ANR-22-EXTR-0002. This work also received support from the European Union's Horizon 2020 research and innovation programme under grant agreement No. 101003469 (XAIDA). PY also acknowledges the support from the French ANDRA and EDF (grant COSTO).

References

Bador, M., Terray, L., Boe, J., Somot, S., Alias, A., Gibelin, A.-L., Dubuisson, B., 2017. Future summer mega-heatwave and record-breaking temperatures in a warmer France climate. Environ. Res. Lett. 12, 074025.

Bastos, A., Fu, Z., Ciais, P., Friedlingstein, P., Sitch, S., Pongratz, J., Weber, U., Reichstein, M., Anthoni, P., Arneth, A., 2020. Impacts of extreme summers on European ecosystems: a comparative analysis of 2003, 2010 and 2018. Philos. Trans. R. Soc. B 375.

Bevacqua, E., Suarez-Gutierrez, L., Jézéquel, A., Lehner, F., Vrac, M., Yiou, P., Zscheischler, J., 2023. Advancing research on compound weather and climate events via large ensemble model simulations. Nat. Commun. 14, 2145.

Carvalho, D., Pereira, S.C., Rocha, A., 2021. Future surface temperatures over Europe according to CMIP6 climate projections: an analysis with original and bias-corrected data. Clim. Change 167, 1–17.

Coles, S., 2001. An introduction to statistical modeling of extreme values. Springer, London, New York, p. 208 pp.,.

D'Andrea, F., Duvel, J.-P., Rivière, G., Vautard, R., Cassou, C., Cattiaux, J., Coumou, D., Faranda, D., Happé, T., Jézéquel, A., Ribes, A., Yiou, P., 2024. Summer Deep Depressions Increase Over the Eastern North Atlantic. Geophys. Res. Lett. 51, e2023GL104435. https://doi.org/10.1029/2023GL104435.

Deser, C., Terray, L., Phillips, A.S., 2016. Forced and internal components of winter air temperature trends over North America during the past 50 years: Mechanisms and implications. J. Clim. 29, 2237–2258.

Domeisen, D.I., Eltahir, E.A., Fischer, E.M., Knutti, R., Perkins-Kirkpatrick, S.E., Schär, C., Seneviratne, S.I., Weisheimer, A., Wernli, H., 2023. Prediction and projection of heatwaves. Nature Reviews Earth & Environment 4, 36–50.

Eyring, V., Bony, S., Meehl, G.A., Senior, C.A., Stevens, B., Stouffer, R.J., Taylor, K.E., 2016. Overview of the Coupled Model Intercomparison Project Phase 6 (CMIP6) experimental design and organization. Geosci. Model Dev. 9, 1937–1958.

Fischer, E.M., Sippel, S., Knutti, R., 2021. Increasing probability of record-shattering climate extremes. Nat. Clim. Chang. 11, 689–695.

Fischer, E.M., Beyerle, U., Bloin-Wibe, L., Gessner, C., Humphrey, V., Lehner, F., Pendergrass, A.G., Sippel, S., Zeder, J., Knutti, R., 2023. Storylines for unprecedented heatwaves based on ensemble boosting. Nat. Commun. 14, 4643.

Florentin, A., Lelievre, M., 2023. Mission d'information et d'évaluation du Conseil de Paris Paris à 50 degrés : s'adapter aux vagues de chaleur. Paris City Council.

Gessner, C., Fischer, E.M., Beyerle, U., Knutti, R., 2021. Very rare heat extremes: quantifying and understanding using ensemble re-initialization. J. Clim. 1–46.

Haylock, M.R., Hofstra, N., Tank, A.M.G.K., Klok, E.J., Jones, P.D., New, M., 2008. A European daily high-resolution gridded data set of surface temperature and precipitation for 1950–2006. J. Geophys. Res. - Atmospheres 113. https://doi.org/10.1029/2008JD010201.

Herrera-Lormendez, P., Douville, H., Matschullat, J., 2023. European summer synoptic circulations and their observed 2022 and projected influence on hot extremes and dry spells. Geophys. Res. Lett. 50 (18) e2023GL104580.

Hersbach, H., Bell, B., Berrisford, P., Hirahara, S., Horányi, A., Muñoz-Sabater, J., Nicolas, J., Peubey, C., Radu, R., Schepers, D., 2020. The ERA5 global reanalysis. Quat. J. Roy. Met. Soc. 146, 1999–2049.

Ibebuchi, C.C., Abu, I.-O., 2023. Characterization of temperature regimes in Western Europe, as regards the summer 2022 Western European heat wave. Clim. Dyn. 61, 3707–3720.

Zhang, Y., Boos, W.R., 2023. An upper bound for extreme temperatures over midlatitude land. Proc. Natl. Acad. Sci. 120 (12), e2215278120.

Kalnay, E., Kanamitsu, M., Kistler, R., Collins, W., Deaven, D., Gandin, L., Iredell, M., Saha, S., White, G., Woollen, J., Zhu, Y., Chelliah, M., Ebisuzaki, W., Higgins, W., Janowiak, J., Mo, K., Ropelewski, C., Wang, J., Leetmaa, A., Reynolds, R., Jenne, R., Joseph, D., 1996. The NCEP/NCAR 40-year reanalysis project. Bull. Amer. Met. Soc. 77, 437–471.

Kerr, R.A., 2005. Atlantic Climate Pacemaker for Millennia past, Decades Hence?, 309. Science.

Maraun, D., Widmann, M., 2018. Statistical downscaling and bias correction for climate research. Cambridge University Press.

Noyelle, R., Yiou, P., Faranda, D., 2023a. Investigating the typicality of the dynamics leading to extreme temperatures in the IPSL-CM6A-LR model. Clim Dyn. https://doi.org/10.1007/s00382-023-06967-5.

Noyelle, R., Zhang, Y., Yiou, P., Faranda, D., 2023b. Maximal reachable temperatures for Western Europe in current climate. Environ. Res. Lett. 18, 094061. https://doi.org/10.1088/1748-9326/acf679.

Parey, S., 2008. Extremely high temperatures in France at the end of the century. Clim. Dyn. 30, 99–112. https://doi.org/10.1007/s00382-007-0275-4.

Philip, S.Y., Kew, S.F., van Oldenborgh, G.J., Anslow, F.S., Seneviratne, S.I., Vautard, R., Coumou, D., Ebi, K.L., Arrighi, J., Singh, R., van Aalst, M., Pereira Marghidan, C., Wehner, M., Yang, W., Li, S., Schumacher, D.L., Hauser, M., Bonnet, R., Luu, L.N., Lehner, F., Gillett, N., Tradowsky, J.S., Vecchi, G.A., Rodell, C., Stull, R.B., Howard, R., Otto, F.E.L., 2022. Rapid attribution analysis of the extraordinary heat wave on the Pacific coast of the US and Canada in June 2021. Earth Syst. Dynam. 13, 1689–1713. https://doi.org/10.5194/esd-13-1689-2022.

Quintana-Segui, P., Le Moigne, P., Durand, Y., Martin, E., Habets, F., Baillon, M., Canellas, C., Franchisteguy, L., Morel, S., 2008. Analysis of near-surface atmospheric variables: Validation of the SAFRAN analysis over France. J. Appl. Meteorol. Climatol. 47, 92–107.

Ragone, F., Wouters, J., Bouchet, F., 2018. Computation of extreme heat waves in climate models using a large deviation algorithm. Proc. Nat. Acad. Sci. 115, 24–29.

IPCC, 2021. Climate Change 2021: The Physical Science Basis. Contribution of Working Group I to the Sixth Assessment Report of the Intergovernmental Panel on Climate Change [Masson-Delmotte, V., P. Zhai, A. Pirani, S.L. Connors, C. Péan, S. Berger, N. Caud, Y. Chen, L. Goldfarb, M.I. Gomis, M. Huang, K. Leitzell, E. Lonnoy, J.B.R. Matthews, T.K. Maycock, T. Waterfield, O. Yelekçi, R. Yu, and B. Zhou (eds.)]. Cambridge University Press, Cambridge, United Kingdom and New York, NY, USA, 2391 pp. https://doi.org/10.1017/9781009157896.

Riahi, K., Van Vuuren, D. P., Kriegler, E., Edmonds, J., O'neill, B. C., Fujimori, S., Bauer, N., Calvin, K., Dellink, R., and Fricko, O.: The Shared Socioeconomic Pathways and their energy, land use, and greenhouse gas emissions implications: An overview, Global environmental change, 42, 153–168, 2017.

Robin, Y., Ribes, A., 2020. Nonstationary extreme value analysis for event attribution combining climate models and observations. Adv. Stat. Climatol. Meteorol. Oceanogr. 6, 205–221.

Röthlisberger, M., Papritz, L., 2023. Quantifying the physical processes leading to atmospheric hot extremes at a global scale. Nat. Geosci. 16, 210–216.

Rousi, E., Kornhuber, K., Beobide-Arsuaga, G., Luo, F., Coumou, D., 2022. Accelerated western European heatwave trends linked to more-persistent double jets over Eurasia. Nat. Commun. 13, 1–11.

Trenberth, K.E., 1997. The definition of El Niño. Bull. Am. Meteorol. Soc. 78, 2771–2778.

Vautard, R., Cattiaux, J., Happé, T., Singh, J., Bonnet, R., Cassou, C., Coumou, D., D'Andrea, F., Faranda, D., Fischer, E., Ribes, A., Sippel, S., Yiou, P., 2023. Heat extremes in Western Europe increasing faster than simulated due to atmospheric circulation trends. Nat. Commun. 14, 6803. https://doi.org/10.1038/s41467-023-42143-3.

von Storch, H., Zwiers, F.W., 2001. Statistical Analysis in Climate Research. Cambridge University Press, Cambridge.

Yin, J., Gentine, P., Slater, L., Gu, L., Pokhrel, Y., Hanasaki, N., Guo, S., Xiong, L., Schlenker, W., 2023. Future socio-ecosystem productivity threatened by compound drought–heatwave events. Nat. Sustainability 6, 259–272.

Yiou, P., Jézéquel, A., 2020. Simulation of extreme heat waves with empirical importance sampling. Geosci. Model Dev. 13, 763–781. https://doi.org/10.5194/gmd-13-763-2020.

Yiou, P., Faranda, D., Thao, S., Vrac, M., 2021. Projected Changes in the Atmospheric Dynamics of Climate Extremes in France. Atmos. 12. https://doi.org/10.3390/atmos12111440.